Physica A 186 (1992) 1–32
North-Holland

PHYSICA A

Fractal landscapes in physics and biology

H. Eugene Stanley

Center for Polymer Studies and Department of Physics, Boston University, Boston, MA 02215, USA

Dedicated to the memory of Satyajit Ray

This article is based upon the Thirtieth Saha Memorial Lecture (delivered on 4 January 1992) and the Fourth Bose Memorial Lecture (delivered on 5 January 1992). I felt deeply touched to have been so honored by invitations to deliver these lectures, especially in view of the list of illustrious predecessors who have held this honor. At the outset I wish to acknowledge that almost all of my work is connected in one way or another to random walks, a topic about which I learned most from the classic 1943 review of the great Indian physicist S. Chandrasekar. I also wish to acknowledge my personal debt to the great culture and music of India, and to the many Indian scholars who have taught me their unique insights into the mysteries of physics. In particular, I wish to dedicate this work to the late Bengali genius Satyajit Ray, whose recent passing has left the world immeasurably poorer. It was my dream while in Calcutta to have the opportunity of meeting this hero of mine, but his ill health at that time prevented our meeting.

1. Introduction

In recent years, a wide range of complex structures of interest to scientists, engineers and physicians have been quantitatively characterized using the idea of a *fractal* dimension: a dimension – usually not an integer – that corresponds in a unique fashion to the geometrical shape under study. The key to this progress is the recognition that many random structures obey a symmetry as striking as that obeyed by regular structures. This "scale symmetry" has the implication that objects look the same on many different scales of observation [1–23]. Nonspecialists are also familiar with fractals. Everyone has seen fractal objects – probably at an early stage in life. Perhaps we once photographed scenery from the back of a train and noticed that the photograph looked the same at all stages of enlargement (fig. 1). Perhaps we noticed that the suburban railway system of Paris has a ramified structure (fig. 2) which in fact turns out to be a fractal object [24]. Perhaps we observed that snow crystals all have the same pattern, each part of a branch being similar to itself. In fact, to "see" something at all –

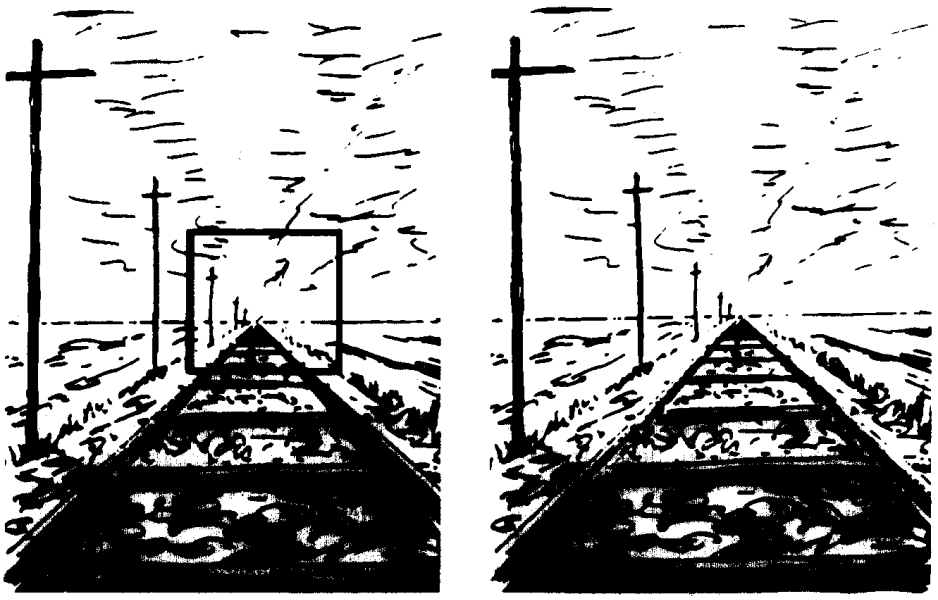

Fig. 1. Schematic illustration of scale invariance for a blow-up of the central portion of a photograph taken from the rear of a train in Oklahoma.

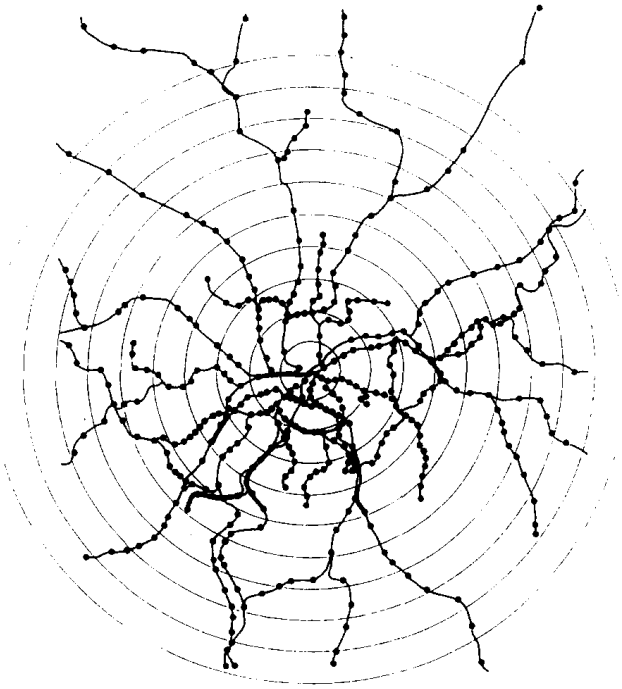

Fig. 2. Sketch of the railway network of the greater Paris area. This includes the R.E.R. and S.N.C.F. systems. After ref. [24].

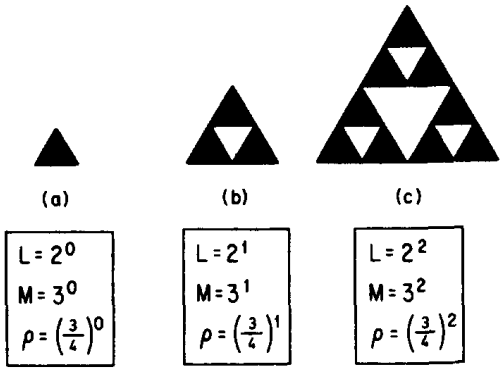

Fig. 3. First few stages in the aggregation rule which is iterated to form a Sierpiński gasket fractal. After ref. [16].

fractal or nonfractal – requires that the nerve cells in the eye's retina send a signal, and these retinal nerve cells are themselves fractal objects.

2. Nonrandom fractals

Fractals fall naturally into two categories, *nonrandom* and *random*. Fractals in physics belong to the second category, but it is instructive to first discuss a much-studied example of a nonrandom fractal – the Sierpiński gasket. We simply iterate a *growth rule*, much as a child might assemble a castle from building blocks. Our basic unit is a triangular-shaped tile shown in fig. 1a, which we take to be of unit *mass* ($M = 1$) and of unit edge *length* ($L = 1$). The Sierpiński gasket is defined – operationally – as an "aggregation process" obtained by a simple iterative process. In stage one, we join three tiles together to create the structure shown in fig. 3b, an object of mass $M = 3$ and edge $L = 2$. The effect of stage one is to produce a unit with a lower density. If we define the density to be

$$\varrho(L) \equiv M(L)/L^2, \tag{1}$$

then the density decreases from unity to 3/4 as a result of stage one.

Now simply iterate – i.e., repeat this rule over and over ad infinitum. Thus in stage two, join together – as in fig. 3c – three of the $\varrho = 3/4$ structures constructed in stage one, thereby building an object with $\varrho = (3/4)^2$. In stage three, join three objects identical to those constructed in stage two. Continue until you run out of tiles (if you are a physicist) or until the structure is infinite (if you are a mathematician!). The result after stage four – with 81 black tiles and 27 + 36 + 48 + 64 white tiles – may be seen in floor mosaics of the church in Anagni, Italy, which was built in the year 1104 (fig. 4). Thus although this fractal is named

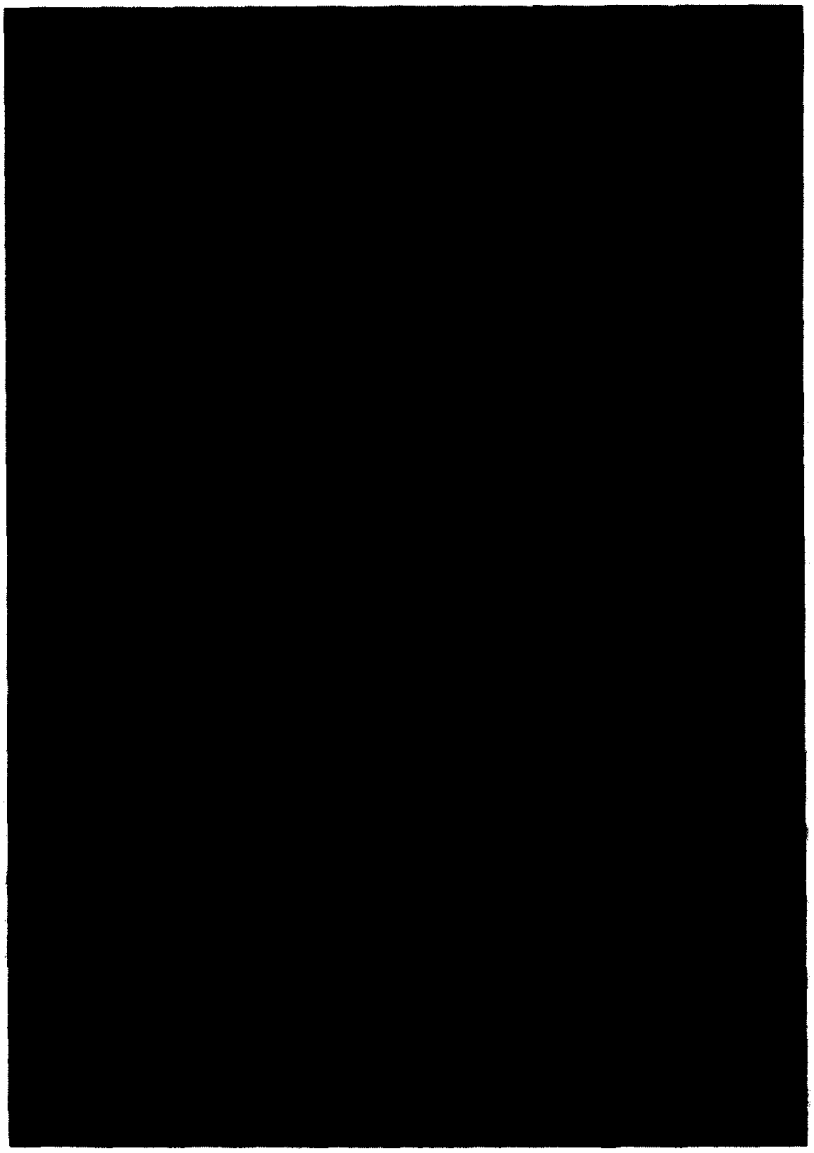

Fig. 4. The floor of the cathedral in Anagni, Italy is adorned with dozens of mosaics, each in the form of a Sierpiński gasket fractal. Shown here is a part of one mosaic, showing the fractal at its fourth stage of iteration. The cathedral and its floor were built in the year 1104 and is possibly the oldest man-made fractal object. (Courtesy of Rachel Stanley, who at the very young age of 10 spotted and photographed this very "old" fractal.)

after the 20th century Polish mathematician W. Sierpiński, it was universally known some eight centuries earlier to every churchgoer of this village!

The citizens of Anagni did not have double-logarithmic graph paper in the 12th century. If they had possessed such a marvelous invention, then they might have plotted the dependence of ϱ on L. They would have found fig. 5, which

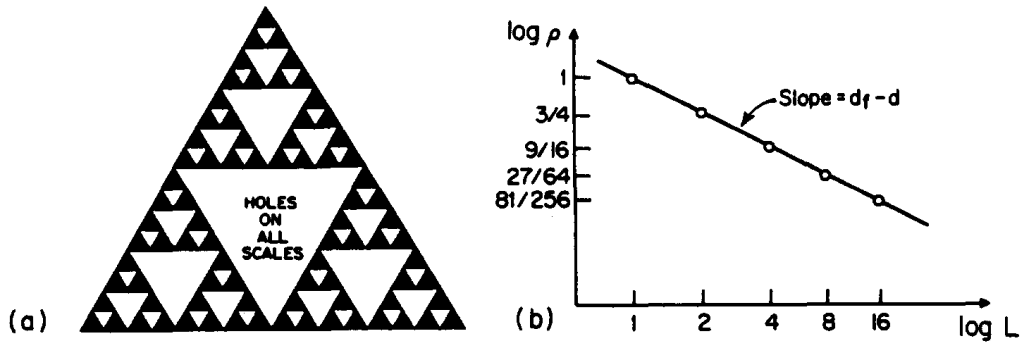

Fig. 5. (a) Sierpiński gasket fractal after four stages of iteration. (b) A log–log plot of ϱ, the fraction of space covered by black tiles, as a function of L, the linear size of the object. After ref. [26].

displays two striking features:
– $\varrho(L)$ decreases monotonically with L, without limit, so that by iterating sufficiently we can achieve an object of *as low a density as we wish*, and
– $\varrho(L)$ decreases with L in a *predictable* fashion – a simple power law.
Power laws have the generic form $y = Ax^{\alpha}$ and, as such, have two parameters, the *amplitude* A and the *exponent* α. The amplitude is not of intrinsic interest, since it depends on the choice we make for the definitions of M and L. The exponent, on the other hand, depends on the process itself – i.e., on the "rule" that we follow when we iterate. Different rules give different exponents. In the present example, the exponent is given by the slope of fig. 5b,

$$\alpha = \text{slope} = \frac{\log 1 - \log(3/4)}{\log 1 - \log 2} = \frac{\log 3}{\log 2} - 2, \tag{2}$$

while $A = 1$ since $\varrho(L) = L^{\alpha}$.

Finally we are ready to define the fractal dimension d_f, through the equation

$$M(L) \equiv AL^{d_f}. \tag{3}$$

If we substitute (3) into (1), we find

$$\varrho(L) = A\, L^{d_f - 2}. \tag{4}$$

Comparing (2) and (4), we conclude that the Sierpiński gasket is indeed a fractal object with fractal dimension

$$d_f = \log 3/\log 2 = 1.58\ldots \quad . \tag{5}$$

Classical (Euclidean) geometry deals with regular forms having a dimension the same as that of the embedding space. For example, a line has $d = 1$, and a square $d = 2$. We say that the Sierpiński gasket has a dimension intermediate

between that of a line and an area – a kind of "fractional" dimension – and hence the term *fractal.*

3. Random fractals

Real systems in nature do not resemble the floor of the Anagni church – in fact, *nonrandom* fractals are rarely found in nature. Nature exhibits numerous examples of objects which by themselves are not fractals but which have the remarkable feature that, if we form a *statistical average* of some property such as the density, we find a quantity that decreases linearly with length scale when plotted on double-logarithmic paper. Such objects are termed *random fractals*, to distinguish them from the nonrandom *geometric fractals* discussed in the previous section.

In his book *Les Atomes*, the French physicist Jean Perrin in 1913 gave a first vivid description of random fractals, using the example of the trail of a Brownian particle. Perrin wrote, "Fresh irregularities appear each time we increase the magnification" [25], which corresponds to finding "holes of all sizes" as in fig. 5. He realized that this finding was remarkably universal – it describes not only the trail of a Brownian particle (fig. 6), but also a range of other natural phenomena. One of these is the coastline of Brittany – Perrin noted that the coastline has a length that increases as the measuring stick used to measure its length gets smaller. Years later, Mandelbrot showed that the fractal dimension d_f provides a quantitative measure of the roughness of such coastlines.

Fig. 7 is a computer simulation of a random walk with a *constraint* that the trail not intersect itself. Note that this walk has holes of all size scales – small holes, big holes, and even bigger holes. The trail of this constrained random walk is a model of a polymer chain – a polymer is a string of smaller molecules called monomers. A monomer itself is *not* a fractal, but a long string of monomers is.

It is a fact that random fractals abound. Almost any object for which randomness is the basic factor determining the structure will turn out to be fractal over some range of length scales – for much the same reason that the random walk is fractal: there is simply nothing in the microscopic rules that can set a length scale so the resulting macroscopic form is "scale-free" ... scale-free objects obey power laws.

4. One random fractal: diffusion limited aggregation

Today, there are roughly of order 10^3 recognized fractal systems in nature, though a decade ago when Mandelbrot's classic *Fractal Geometry of Nature* [1]

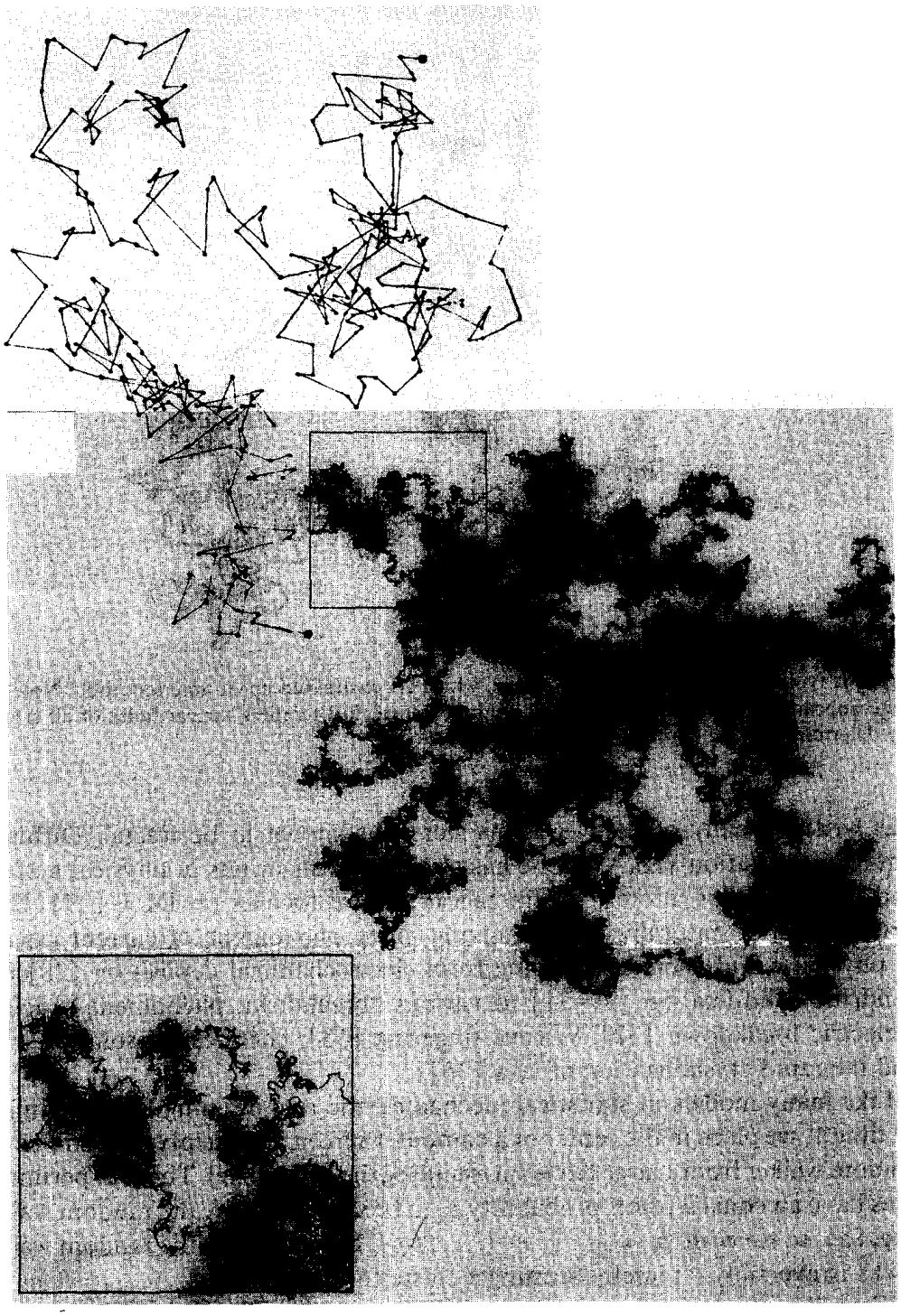

Fig. 6. At the top appears the original document, hand-drawn by Jean Perrin, showing the actual random motion at successive moments of a tiny Brownian particle observed under a microscope [25]. The fractal nature of a "random walk" is seen more clearly from the lower image, generated on a high-speed modern computer. This model is defined by the rule that a walker randomly chooses each step to be North, East, South or West with equal probability. Note that a magnification of a small part of the walk (see inset) has the same appearance as the original pattern. Courtesy of B. Duplantier. After ref. [22].

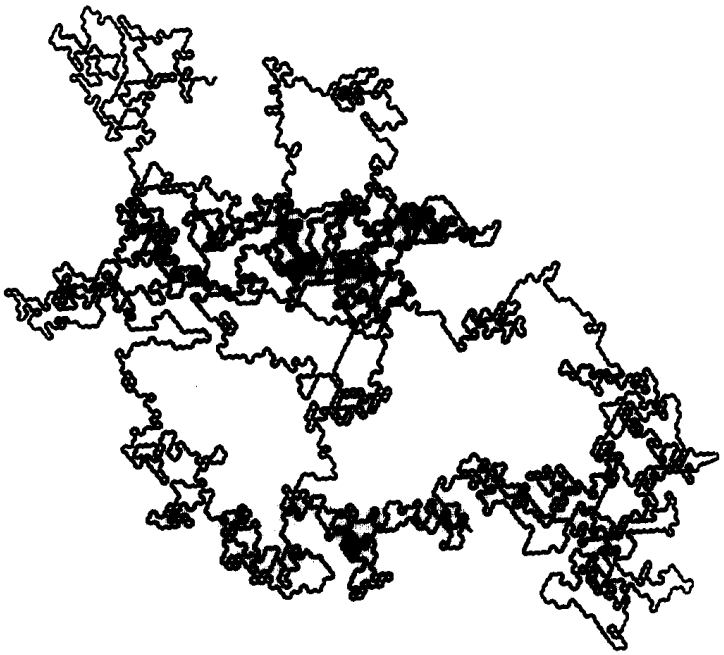

Fig. 7. A typical random walk of 5000 steps, which is constrained not to intersect itself. Note that there appear "holes of all sizes" in this random fractal, just as there appear holes of all sizes in the deterministic fractal of fig. 5. Courtesy of P. Poole.

was written, many of these systems were not known to be fractal. Diffusion limited aggregation (DLA) alone has about 50 realizations in physical systems and much current interest on fractals in nature focuses on DLA [27]. DLA structures arise naturally when studying many phenomena of current interest to physicists and chemists, ranging from electrochemical deposition [28] and dendritic solidification [29–31] to various "breakdown phenomena" such as dielectric breakdown [32], viscous fingering [33], chemical dissolution [34] and the rapid crystallization of lava [35].

Like many models in statistical mechanics, the rule defining DLA is simple. At time 1, we place in the center of a computer screen a white pixel, and release a random walker from a large circle surrounding the white pixel. The four perimeter sites have an equal a priori probability p_i to be stepped on by the random walker (fig. 8a), so we write $p_i = \frac{1}{4} \quad (i = 1, \ldots, 4)$. The rule is that the random walker sticks irreversibly – thereby forming a cluster of mass $M = 2$.

There are now six possible sites, called *growth sites* (fig. 8b), but the probabilities p_i are *no longer* all identical: each of the growth sites of the two tips has growth probability $p_{\max} \cong 0.22$, while each of the four growth sites on the sides has growth probability $p_{\min} \cong 0.14$. Since a site on the tip is 50% more likely to grow than a site on the sides, the next site is more likely to be added to the tip

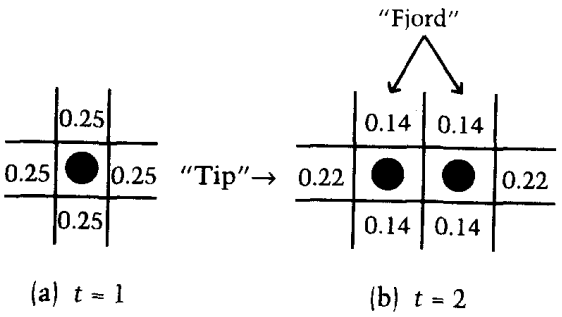

Fig. 8. (a) Square lattice DLA at time $t = 1$, showing the four growth sites, each with growth probability $p_i = 1/4$. (b) DLA at time $t = 2$, with 6 growth sites, and their corresponding growth probabilities p_i. After ref. [21].

– it is like capitalism, in that the rich get richer.

If the DLA growth rule is simply iterated, then we obtain a large cluster characterized by a range of growth probabilities that spans several orders of magnitude – from the tips to the fjords. Fig. 9 shows such a large cluster, where each pixel is shaded according to the time it was added to the aggregate. From the fact that the "last to arrive" particles are never found to be adjacent to the "first to arrive" particles, we conclude that the p_i for the growth sites on the tips must be vastly larger than the p_i for the growth sites in the fjords.

Recently, several phenomena of *biological* interest have attracted the attention of DLA aficionados. These include the growth of bacterial colonies [36], the retinal vasculature [37], neuronal outgrowth [38] (fig. 10), and the classic unresolved puzzle of how HCl, secreted at the base of gastric glands by parietal cells, traverses the mucus layer to reach the lumen without acidifying the mucus layer. The intriguing possibility that flow of HCl through mucus may involve viscous fingering has received support by recent experiments demonstrating that injection of HCl through solutions of pig gastric mucin produces fingering patterns which are strongly dependent on the pH, mucin concentration, and acid flow rate [39]. Above pH 4, discrete fingers are observed, while below pH 4, HCl neither penetrates the mucin solution nor forms fingers. At low mucin concentrations, tip-splitting fingers develop, while at mucin concentrations approaching those that occur in the mammalian stomach, tip-splitting fingers are replaced by 'dendritic' fingers which form narrow channels through the mucin. These results suggest that HCl secreted by the gastric gland can penetrate the mucus gel layer (pH 5–7) through narrow fingers, whereas HCl in the stomach interior (pH 2) is prevented from either diffusive or convective return to the epithelium by the high viscosity of gastric mucus gel on the stomach interior.

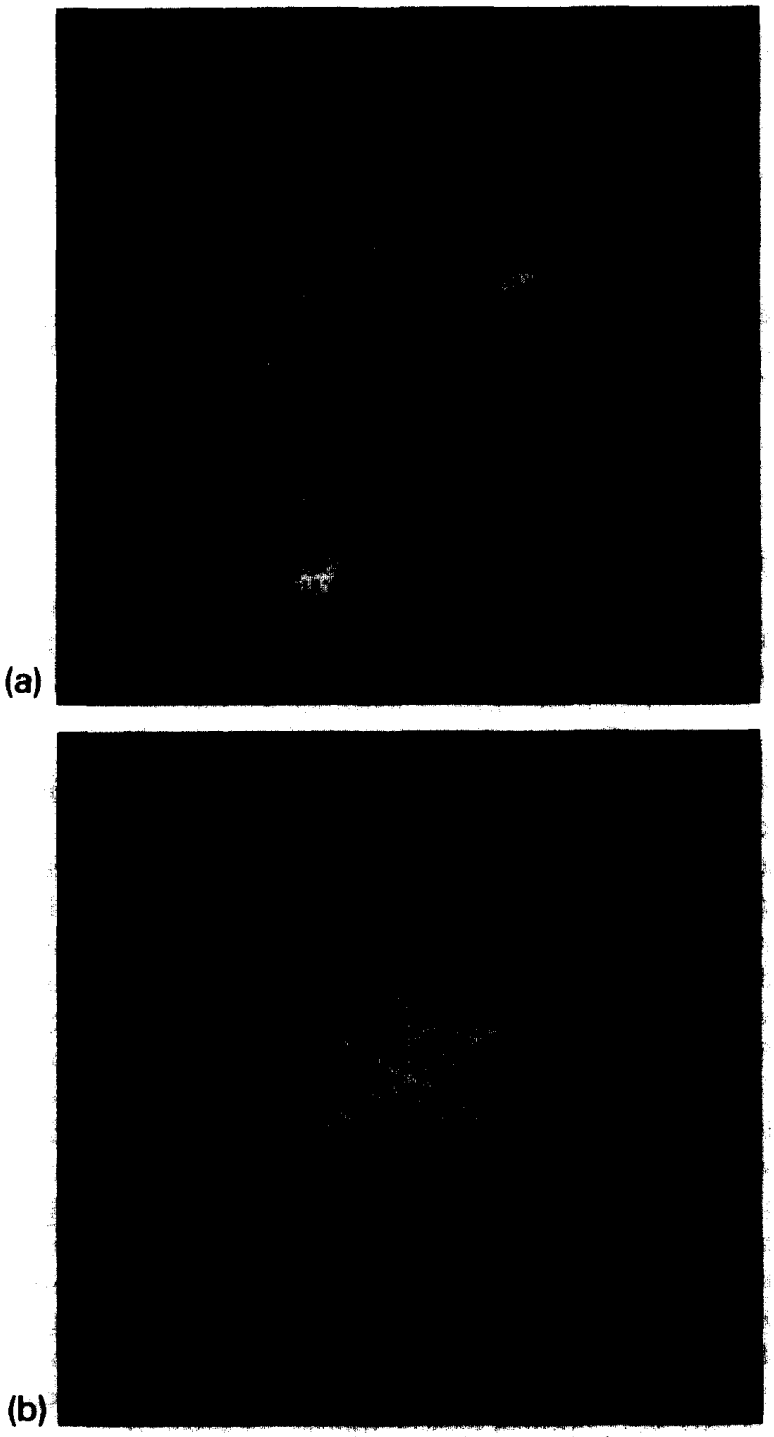

Fig. 9. (a) Large DLA cluster on a square lattice. Each cluster site is shaded according to the time which the site joined the cluster. (b) Same cluster, except that now noise reduction and lattice anisotropy are present, and the cluster takes on a general resemblance to a snowflake. After ref. [29].

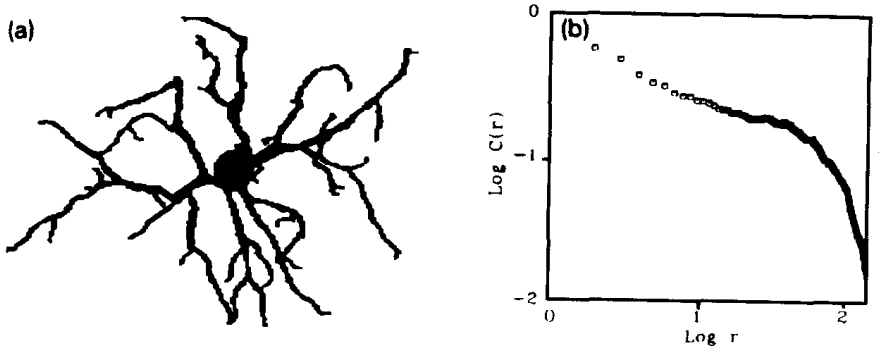

Fig. 10. Typical retinal neuron and its fractal analysis. After ref. [38].

5. Models and their "variants"

In this and the following section, we shall make the case that if one seeks to understand completely the diffusion-limited aggregation (DLA) model, then one may gain insight into the role of fluctuations in a range of systems described by DLA, including fluid mechanical systems, as well as in dendritic solidification. The detailed descriptions of some such systems requires suitably chosen variants, such as DLA with anisotropy and noise reduction.

We first argue that we can approach these experimental subjects of classic difficulty with the same spirit that has been used in recent years to approach problems associated with phase transitions and critical phenomena [40,41]. This approach is to carefully choose a microscopic model system that captures the essential physics underlying the phenomena at hand, and then study this model until we understand "how the model works". Then we reconsider the phenomena at hand, to see if an understanding of the model leads to an understanding of the phenomena. Sometimes the original model is not enough, and a *variant* is needed, and we shall see that this is the case here also. Fortunately, however, we shall see that the same underlying physics is common to the model and its variants.

5.1. Archetype 1: the Ising model and its variants

We begin, then, with the classic Ising model [42]. Over 1000 papers have been published on this model, but only since 1977 have we known that if one understands the Ising model thoroughly, one understands the essential physics of many materials, since they are simply *variants* of the Ising model. For example, a large number of systems are related to special cases of the n-vector model, which in turn is a Ising model in which the spin variable $\boldsymbol{s}$ has not one component but rather n separate components s_j: $\boldsymbol{s} \equiv (s_1, s_2, \ldots, s_n)$.

The Ising model solves the puzzle of how it is that nearest-neighbor interactions of *microscopic* length scale 1 Å "propagate" their effect cooperatively to give

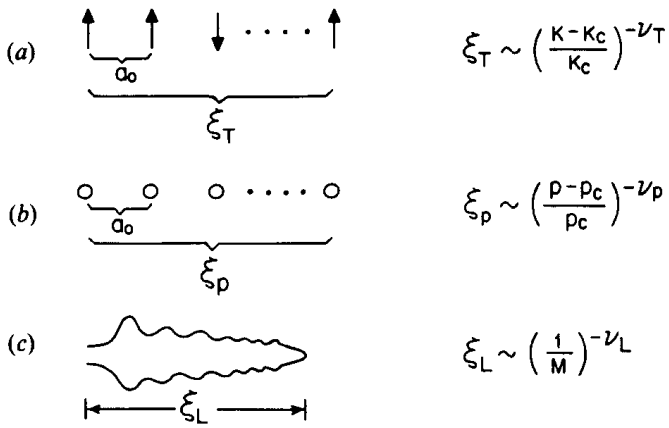

Fig. 11. Schematic illustration of the analogy between: (a) the Ising model, which has fluctuations in spin orientation *on all length scales* from the microscopic scale of the lattice constant a_0 up to the macroscopic scale of the thermal correlation length ξ_T; (b) percolation, which has fluctuations in characteristic size of clusters *on all length scales* from a_0 up to the diameter of the largest cluster – the pair connectedness length ξ_p; and (c) the DLA problem, whose clusters have fluctuations *on all length scales* from the microscopic length $d_0 = \gamma/L$ (γ is the surface tension and L the latent heat) up to the diameter of the cluster ξ_L. Also shown, on the right side, is the analogy between the scaling behavior of the three length scales ξ_T, ξ_p, and ξ_L.

rise to a correlation length ξ_T of *macroscopic* length scale near the critical point (fig. 11a). In fact, ξ_T increases without limit as the coupling $K \equiv J/kT$ increases to a critical value $K_c \equiv J/kT_c$,

$$\xi_T \sim \mathcal{A}\left(\frac{K - K_c}{K_c}\right)^{-\nu_T}. \tag{6}$$

The "amplitude" $\mathcal{A}$ has a numerical value on the order of the lattice constant a_0. A snapshot of an Ising system shows that there are fluctuations on all length scales from a_0 (≈ 1 Å) to ξ_T (which can be from 10^2–10^4 Å in a typical experiment). Direct experimental evidence of this fact is shown in fig. 12, which is a snapshot of a system belonging to the Ising universality class which is illuminated by a beam of visible light. The fact that this light is strongly scattered ("critical opalescence") implies that there must be density fluctuations of a magnitude comparable to the wavelength of the light.

5.2. *Archetype 2: random percolation and its variants*

In percolation [41], one randomly occupies a fraction p of the sites of a d-dimensional lattice (the case $d = 1$ is shown schematically in fig. 11b). Again, phenomena occurring on the local 1 Å scale of a lattice constant are "amplified" near the percolation threshold $p = p_c$ to a macroscopic length ξ_p.

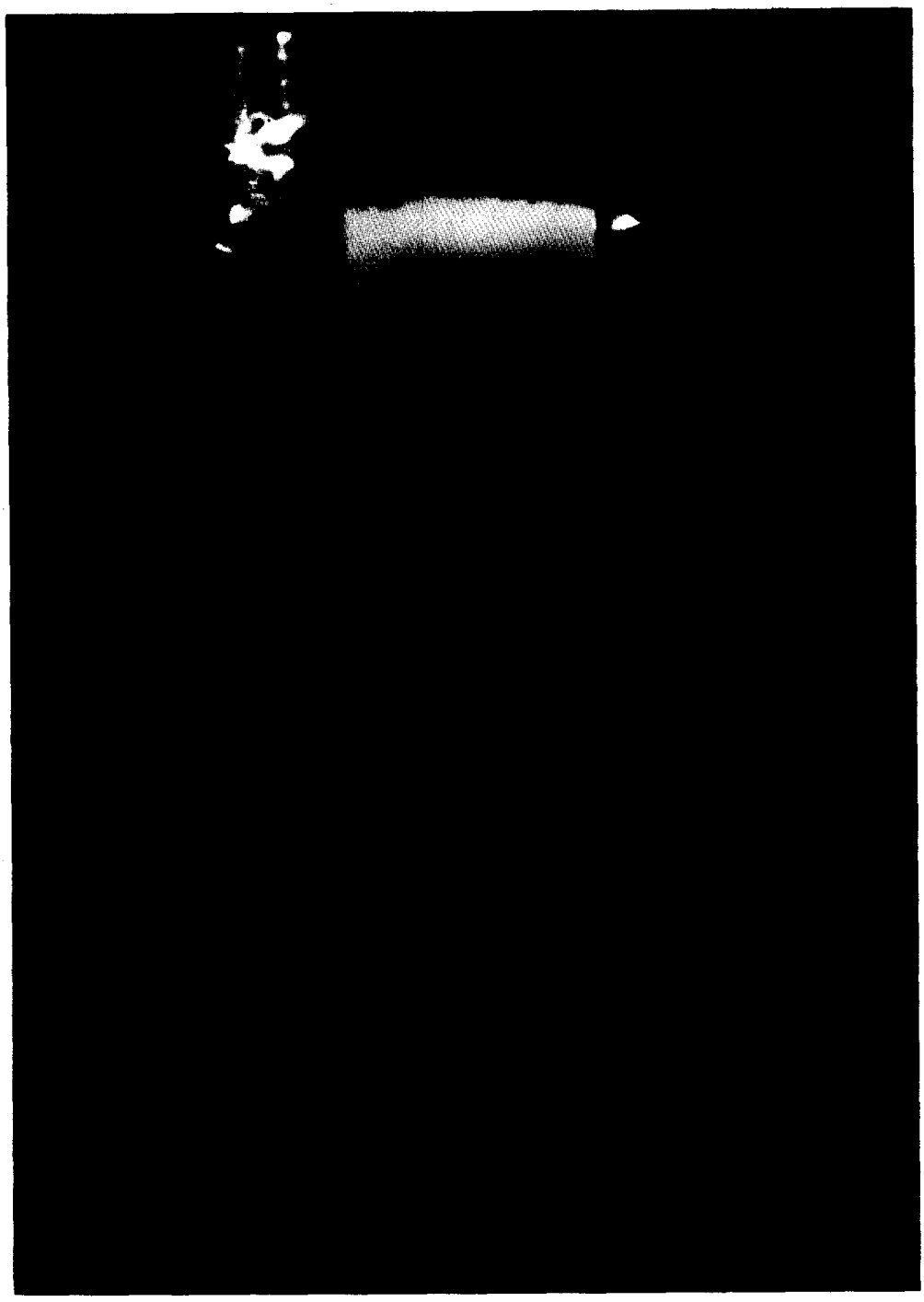

Fig. 12. Behavior of the critical binary mixture cyclohexane-aniline (courtesy of R. A. Ferrell).

Here p plays the role of the coupling constant K of the Ising model. When p is small, the characteristic length scale is comparable to 1 Å. However when p approaches p_c, there occur phenomena on all scales ranging from a_o to ξ_p, where ξ_p increases without limit as $p \to p_c$,

$$\xi_p \sim \mathcal{A}\left(\frac{p - p_c}{p_c}\right)^{-\nu_p}. \tag{7}$$

Again, the amplitude $\mathcal{A}$ is roughly a lattice constant ($\approx$ 1 Å).

Each phenomenon of thermal critical phenomena has a corresponding analog in percolation, so that the percolation problem is sometimes called a geometric or *connectivity* critical phenomenon. Any connectivity problem can be understood by starting with pure random percolation and then adding interactions. Thus, for example, we understand why the critical exponents describing the divergence to infinity of various geometrical quantities (such as ξ_p) are the same regardless of whether the elements interact or are noninteracting [41]. Similarly, the same connectivity exponents are found regardless of whether the elements are constrained to the sites of a lattice or are free to be anywhere in a continuum [41].

The range of systems for which connectivity concepts are relevant is remarkably large. Examples of recent interest in our research group include the hydrogen bonded network of liquid water (see fig. 13) and processes that occur under conditions in which a physical gelation phenomenon occurs *simultaneously* with a phase separation phenomenon (fig. 14).

5.3. *Archetype 3: the Laplace equation and its variants*

Just as variations in the Ising and percolation problems were found to be sufficient to describe a rich range of thermal and geometric critical phenomena, so we have found that variants of the original Laplace equation $\nabla^2\phi = 0$ that enters in the mathematical description of DLA are useful in describing puzzling patterns in fluid mechanics, dendritic growth, and various breakdown phenomena.

In the Ising model, we place a spin on each pixel (site) of a lattice. In percolation we allow each pixel to be occupied or empty. In fluid mechanics, we assign a number – call it ϕ – to each pixel. We might think of ϕ as being the pressure or chemical potential at this region of space.

The spins in an Ising model interact with their neighbors. Hence the state of one Ising pixel depends on the state of all the other pixels in the system – up to a length scale given by the thermal correlation length ξ_T. The "global" correlation between distant pixels in an Ising simulation arises from the fact that neighboring pixels at i and j have a "local" exchange interaction J_{ij}. Similarly, the correlation in connectivity between distant pixels in the percolation problem

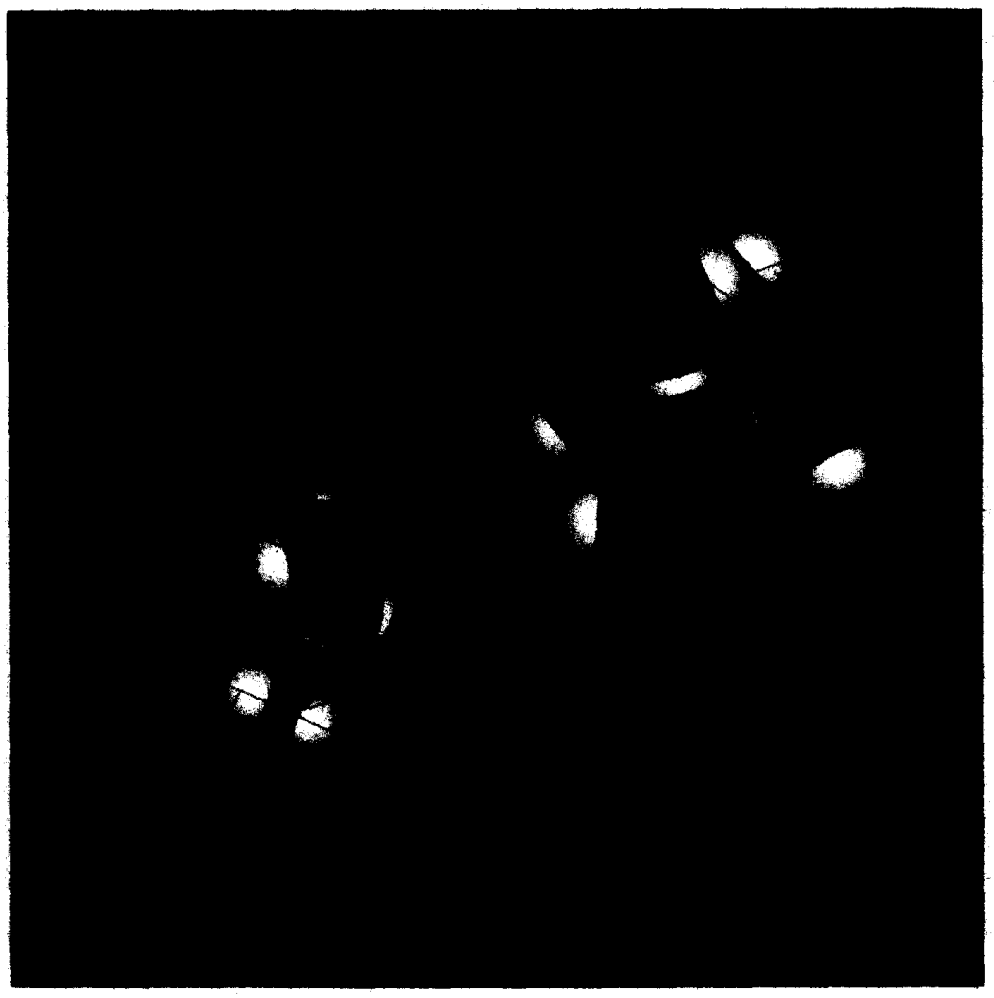

Fig. 13. Snapshot of the connected network of liquid water. The enlargements indicate two different local geometries. One enlargement shows the configuration associated with low mobility, a conventional four-bonded molecule; here each of the two protons and two lone pairs of the central water molecule are oriented directly at four adjacent neighbors. The other enlargement shows a five-bonded configuration associated with higher mobility. Courtesy of B. Ostrovsky [43].

arises from the "propagation" of local connectivity between neighboring pixels. In fluid mechanics, the pressure on each pixel is correlated with the pressure at every other pixel because the pressure obeys the Laplace equation.

One can calculate an equilibrium Ising configuration by "passing through the system with a computer" and flipping each spin with a probability related to the Boltzmann factor. Similarly, one can calculate the pressure at each pixel by "passing through the system" and re-adjusting the pressure on each pixel in accord with the Laplace equation. If we were to arbitrarily flip the configuration

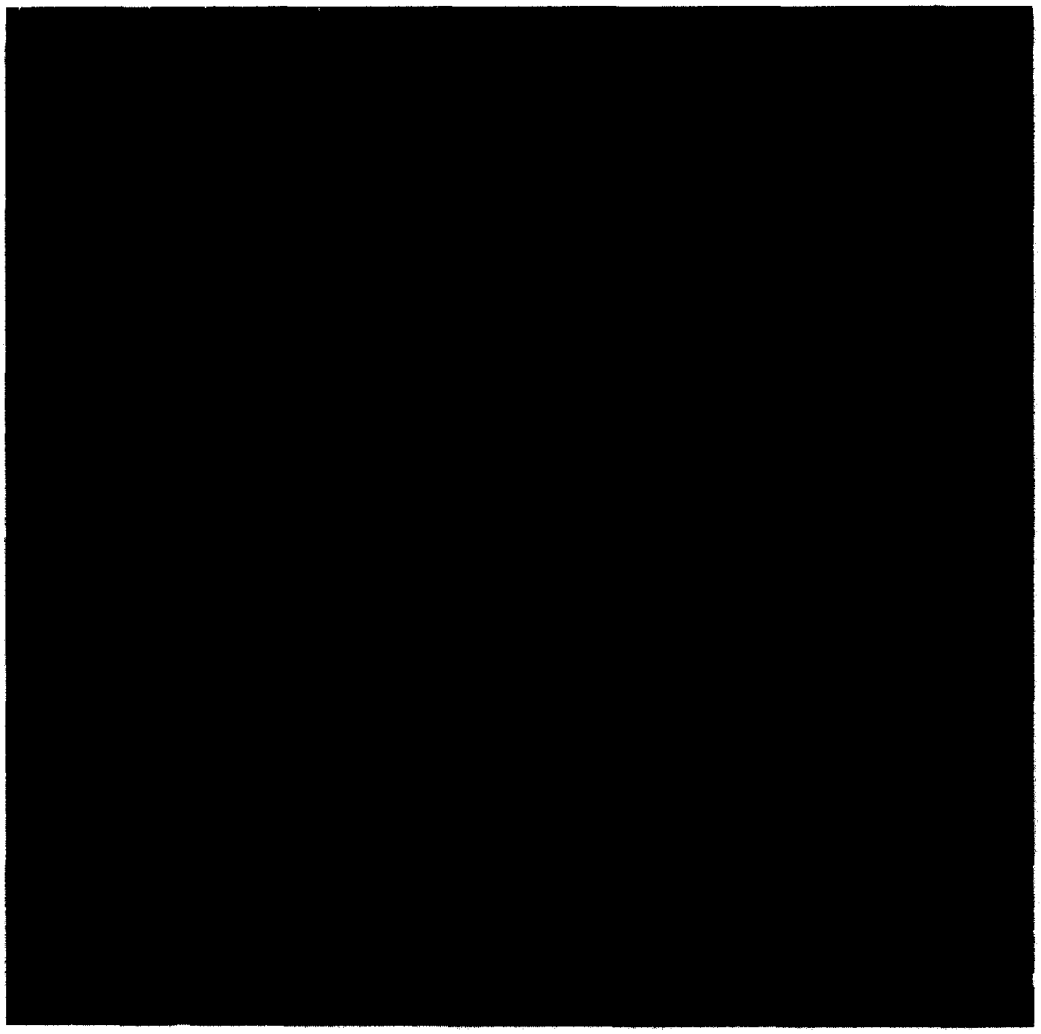

Fig. 14. A model of a cross-linking polymer system quenched into the two-phase region. Note that this system has the potential to be a "filter" of a mesh size given by the characteristic spacing between the polymer strands. Courtesy of S. Glotzer [44].

of a single pixel in the Ising problem (from $+1$ to -1), we would significantly influence the configuration of the system out to a length scale on the order of ξ_T. Similarly, if we were to arbitrarily impose a given pressure on a single point of a system obeying the Laplace equation, we would drastically change the resulting pattern out to a length scale that we shall call ξ_L.

Does ξ_L obey a "scaling form" analogous to eqs. (6) and (7) obeyed by the functions ξ_T and ξ_p for the Ising model and percolation? We believe that the answer to this question is "yes", although our ideas on this subject remain somewhat tentative and subject to revision.

In both thermal critical phenomena and percolation the length L introduced when we have a finite system size scales the same as the correlation lengths ξ_T (or ξ_p). Hence for DLA we expect that there will be fluctuations on length scales up to ξ_L, where ξ_L itself increases with the cluster mass according to

$$\xi_L \sim \mathcal{A}\left(\frac{1}{M}\right)^{-\nu_L} \qquad \left(d_f \equiv \frac{1}{\nu_L} = \text{fractal dimension}\right). \tag{8}$$

Here the amplitude $\mathcal{A}$ is again on the order of 1 Å. Note that (8) is analogous to (6) and (7) if we think of $M \to \infty$ as being analogous to $K \to K_c$. Note also that $\nu_L = 1/d_f$ plays the role of the critical exponents ν_T and ν_p of (6) and (7). Suppose one tests this idea, qualitatively, by examining the largest DLA clusters in detail. One finds that indeed there are fluctuations in mass on length scales less than, say, the width W of the side branches. If one makes a log–log plot of W against mass M, one finds the same slope $1/d_f$ that one finds when one plots the diameter against M [29].

6. Applications of DLA to dendritic growth

6.1. Fluid models of dendritic growth

By analogy with the Ising model and its variants, we can modify DLA to describe a variety of phenomena of interest in fluid mechanics. One of the most intriguing of these concerns a variation of the viscous fingering phenomenon in which anisotropy is present. Ben-Jacob et al. [45] imposed this anisotropy by scratching a lattice of lines on their Hele-Shaw cell. They found patterns that strongly resemble snow crystals! If viscous fingers are described by DLA, then can the Ben Jacob patterns be described by DLA with imposed anisotropy?

Nittmann and Stanley [29] attempted to answer this question – specifically, they attempted to reproduce the Ben-Jacob patterns with suitably modified DLA. A scratch in a Hele-Shaw cell means that the plate spacing b is increased along certain directions, and the permeability coefficient k relating growth velocity to ∇P is proportional to b^2 ($k \propto b^2$). Hence Nittmann and Stanley calculated DLA patterns for the case in which there was imposed a periodic variation in the k, and found patterns resembling snowflakes (fig. 9b).

6.2. Dendritic solid patterns: "snow crystals"

Of course, real dendritic growth patterns (such as snow crystals) do not occur in an environment with periodic fluctuations in $k(x, y)$. Rather, the *global*

asymmetry of the pattern arises from the *local* asymmetry of the constituent water molecules. Can this local asymmetry give rise to global asymmetry? Buka et al. [45] replaced the Ben-Jacob experiment (isotropic fluid, anisotropic cell) by the reverse: isotropic cell but anisotropic fluid!

To accomplish this, they used a nematic liquid crystal for the high viscosity fluid. Thus the analog of the water molecules in a snow crystal are the rod-shaped anisotropic molecules of a nematic. This experiment shows that the underlying anisotropy can as well be in the fluid as in the environment.

Snow crystal formation is thought to involve mainly the aggregation of tiny ice particles and droplets of supercooled water [46–49]. To the extent that snow crystals grow by adding water molecules previously in the vapor or liquid phase, the growth rate is thought to be limited by the diffusion away from the growing snow crystal of the latent heat released by these phase changes. Under conditions of small Péclet number, the diffusion equation describing the space and time dependence of the temperature field reduces to the Laplace equation. Thus a reasonable starting point is DLA, independent of whether we wish to focus on particle aggregation, heat diffusion, or both.

While the various deterministic models of snow crystals produce patterns that are much too "symmetric", the DLA approach suffers from the opposite problem: DLA patterns are too "noisy". That DLA is too noisy has long been recognized as a defect of this otherwise physically appealing model. Recently, an approach has been proposed [31] that retains the "good" features of DLA and at the same time produces patterns that resemble real (random) snow crystals. We introduce controlled amounts of noise reduction. We do not explicitly introduce anisotropy – the only anisotropy present is the six-fold anisotropy arising from the underlying triangular lattice.

The patterns obtained [31] have the same general features for all values of s greater than about $s = 100$. The fjords between the 6 main branches contain much empty space; some snow crystals have such wide "bays" but some do not. A better model would seem to require some tunable parameter that enables the complete range of snow crystal morphologies to be generated. One such parameter, η, has the desired effect of reducing the difference in the ratio of the growth probabilities between the tips and fjords. Specifically, we relate by the rule $p_i \propto (\nabla\phi)^\eta$ the growth probability p_i (the probability that perimeter site i is the next to grow) to the potential ϕ.

We used η to tune the balance between tip growth and fjord growth and found growth patterns that resemble better the wide range of snow crystal morphologies that have been experimentally observed (fig. 15). Moreover, our values for d_f agreed with values we obtained by digitizing photographs of experimentally observed snow crystals [31]. We found that the effect of tuning a surface tension parameter σ is to thicken the side branches, to round the sharper points of the pat-

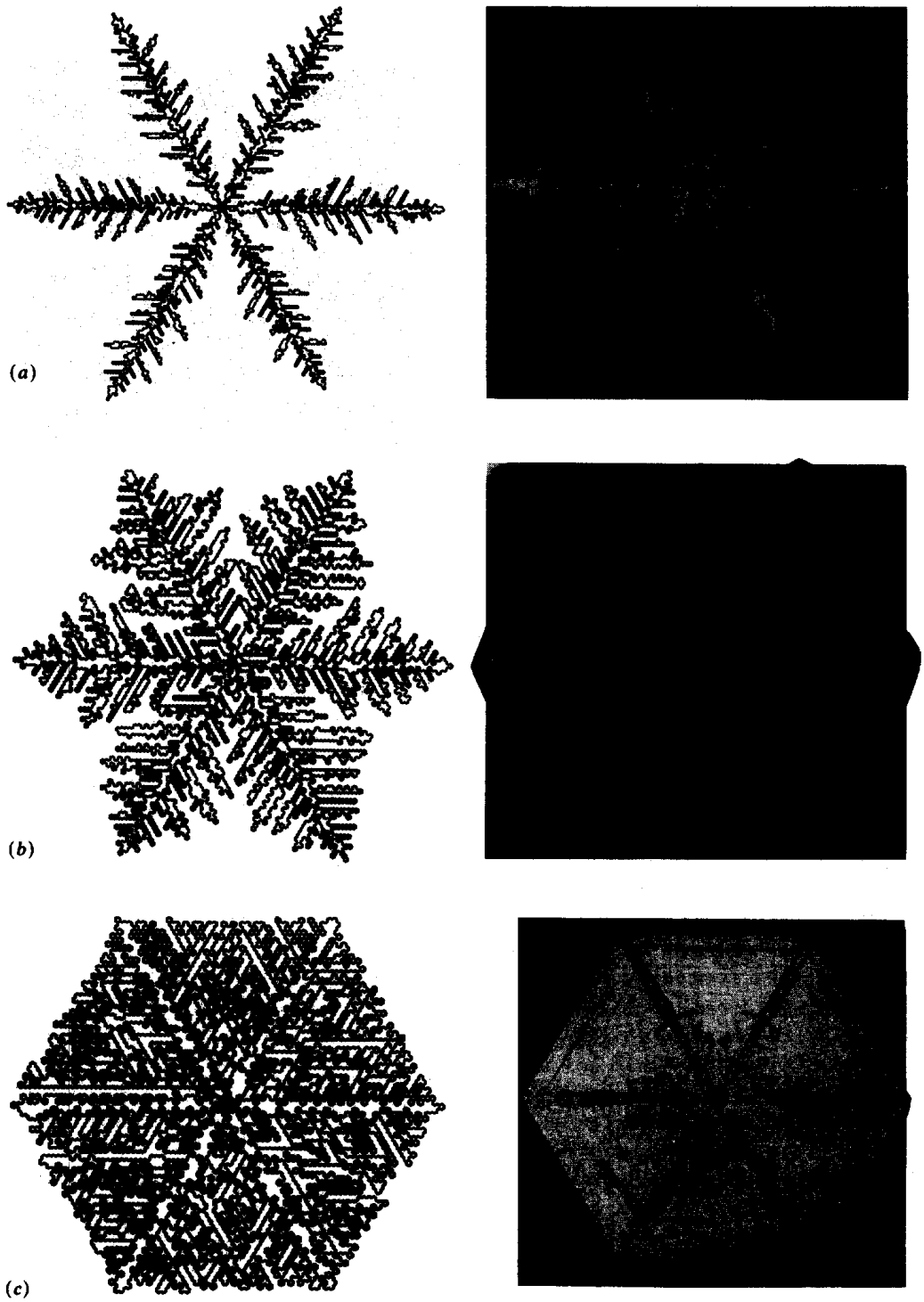

Fig. 15. Comparison between photographs of real snow crystals and some typical DLA computer simulations with 4000 particles and a noise reduction parameter value $s = 200$. (a) $\eta = 1$ ($d_f \cong 1.5$), (b) $\eta \cong 0.5$ ($d_f \cong 1.85$), and (c) $\eta = 0.05$ ($d_f \cong 2$). The *same* values of d_f are found for the experimental patterns shown. After ref. [31].

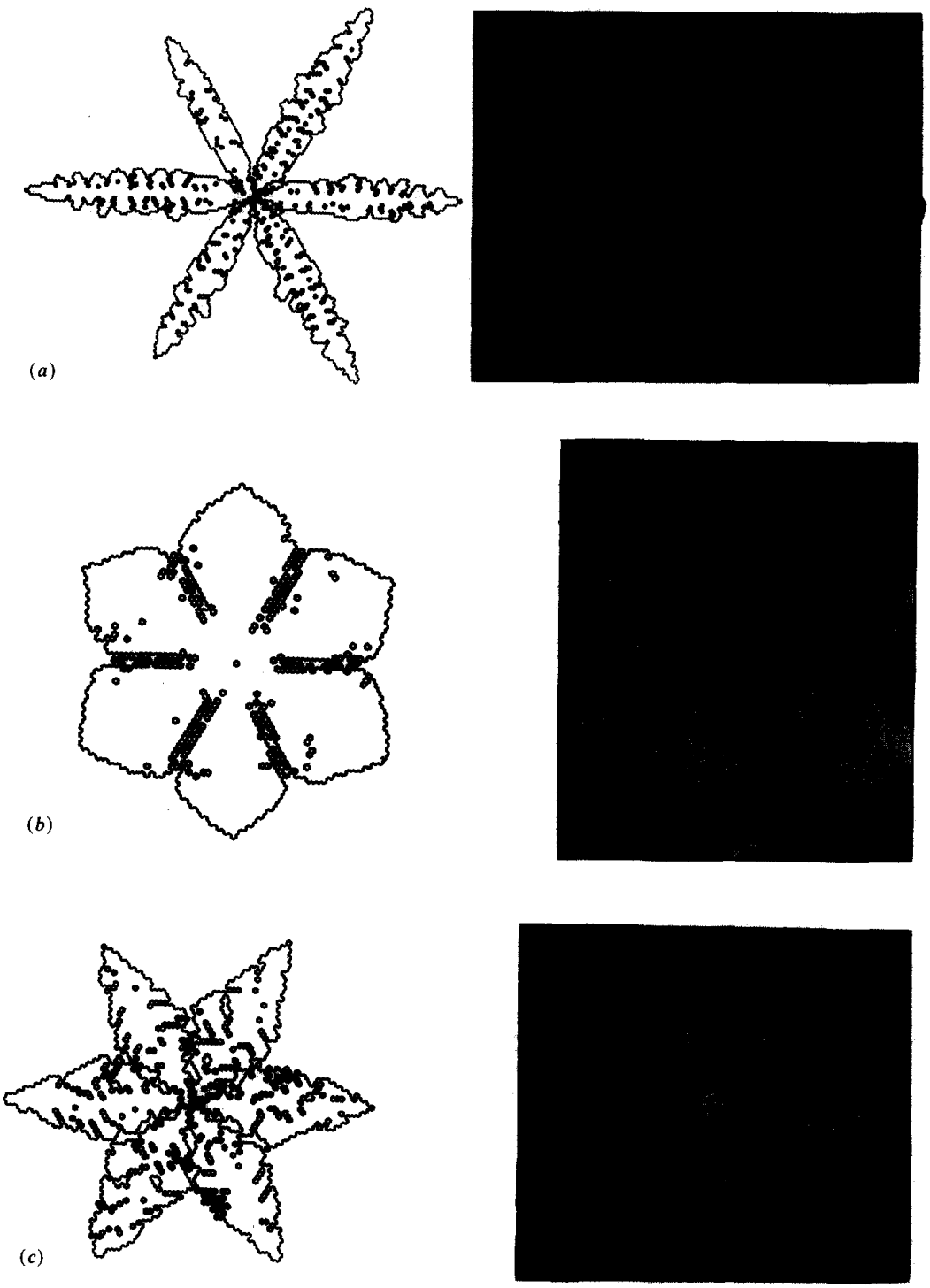

Fig. 16. Comparison between photographs of real snow crystals and some typical DLA computer simulations with non-zero surface tension σ. As in fig. 15, $s = 200$. (a) $\eta = 1.0$ and $\sigma = 0.1$, (b) $\eta = 0.5$ and $\sigma = 0.5$, and (c) $\eta = 0.1$ and $\sigma = 0.2$. After ref. [31].

tern, and to fill in the tiny holes that are present even for small values of η (fig. 16).

6.3. *Dendritic solid patterns: growth of NH_4Br*

Dendritic crystal growth has been a field of immense recent progress, both experimentally and theoretically. In particular, Dougherty et al. [50] have made a detailed analysis of stroboscopic photographs, taken at 20 s intervals, of dendritic crystals of NH_4Br (fig. 17a). Simulations based on DLA are shown in fig. 17b. After each 333 particles are added, a contour has been drawn. The patterns obtained strongly resemble the experimental patterns of fig. 17a. Side branching arises from the fact that an approximately flat interface in the DLA problem grows "trees" (which resemble "bumps" in the presence of noise reduction); these compete for the incoming flux of random walkers. If one "tree" gets ahead, it has a further advantage for the next random walker and so gets ahead still more. Thus some side branches grow while others do not. The patterns we obtain are reasonably independent of details of the simulation in that similar patterns are obtained when we vary the surface tension parameter σ over a modest range; we can also alter the boundary conditions of the model with some latitude and even allow for nonlinearity in the growth process ($\eta \neq 1$).

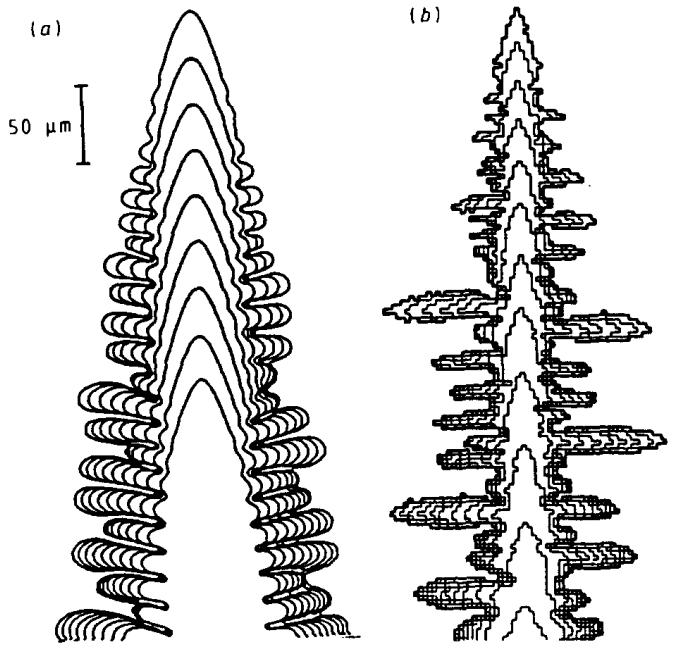

Fig. 17. (a) Experimental pattern of dendritic growth, measured for NH_4Br by Dougherty et al. [50]. (b) DLA simulation with noise reduction parameter $s = 200$. After ref. [30].

7. Long-range correlations in nucleotide sequences

Before concluding, I wish to offer two examples of recent work concerning biological applications of fractals. The first of these [51] represents an extension of our group's work on "correlated randomness" (random systems with long-range correlations) [52]. DNA nucleotide sequences have been analyzed using models – such as an n-step Markov chain – which incorporate the possibility of *short-range* nucleotide correlations [53]. We are using a novel method for studying the stochastic properties of nucleotide sequences by constructing a 1:1 map of the nucleotide sequence onto a walk – which we term a DNA walk. We used this mapping to provide a quantitative measure of the correlation between nucleotides over long distances along the DNA chain. We discovered in the nucleotide sequence a remarkably *long-range* power law correlation that is significant because it implies a new scale invariant property of DNA. We found such long-range correlations in intron-containing genes and in non-transcribed regulatory DNA sequences, but not in cDNA sequences or intronless genes.

For the conventional one-dimensional random walk model, a walker moves either up ($u(i) = +1$) or down ($u(i) = -1$) one unit length for each step i of the walk [54]. The DNA walk is defined by the rule that the walker steps up ($u(i) = +1$) if a pyrimidine occurs at position a linear distance i along the DNA chain, while the walker steps down ($u(i) = -1$) if a purine occurs at position i. The question we ask is whether such a walk displays only short-range correlations (as in an n-step Markov chain) or long-range correlations (as in critical phenomena and other scale-free "fractal" phenomena).

This DNA walk provides a novel graphical representation for each gene and permits the degree of correlation in the nucleotide sequence to be directly visualized (fig. 18). It naturally motivates a quantification of this correlation by calculating the "net displacement" $y(\ell)$ of the walker after ℓ steps, which is the sum of the unit steps $u(i)$ for each step i, $y(\ell) \equiv \sum_{i=1}^{\ell} u(i)$.

An important statistical quantity characterizing any walk is the root mean square fluctuation $F(\ell)$ about the average of the displacement. For the case of an uncorrelated walk, the direction of each step is independent of the previous steps. For the case of a correlated random walk, the direction of each step depends on the history ("memory") of the walker.

The calculation of $F(\ell)$ can distinguish three possible types of behavior. (i) If the nucleotide sequence were random, then $F(\ell) \sim \ell^{1/2}$ (as expected for a *normal* random walk). (ii) If there were a local correlation extending up to a characteristic range (such as in Markov chains), then *the asymptotic behavior* $F(\ell) \sim \ell^{1/2}$ *would be unchanged from the purely random case.* (iii) If there is no characteristic length (i.e., if the correlation were "infinite-range"), then the

fluctuations will be described by a power law

$$F(\ell) \sim \ell^{\alpha}, \tag{9}$$

with $\alpha \neq 1/2$.

The power-law form of eq. (9) implies a self-similar (fractal) property in the DNA walk representation. To visualize this finding, one can magnify a segment of the DNA walk to see if it resembles (in a statistical sense) the overall pattern. Fig. 19(top) shows the DNA walk representation of a gene while figs. 19(middle and bottom) show successive magnifications of the central portion. Note the similar fluctuation behavior on the two different length scales shown.

We made double-logarithmic plots of the mean square fluctuation $F(\ell)$ as a function of the linear distance ℓ along the DNA chain for representative genomic and cDNA sequences across the phylogenetic spectrum. In addition, we analyzed other sequences encoding a variety of other proteins as well as regulatory DNA sequences. We discovered that remarkably long-range correlations ($\alpha > 1/2$) are characteristic of intron-containing genes and non-transcribed genomic regulatory elements. In contrast, for cDNA sequences and genes without introns, we find that $\alpha \cong 1/2$ indicating no long-range correlation. Thus, the calculation of $F(\ell)$ for the DNA walk representation provides a new, *quantitative* method to distinguish genes with multiple introns from intron-less genes and cDNAs based solely on their statistical properties. The finding of long-range correlations in intron-containing genes appears to be independent of the particular gene or the encoded protein – it is observed in genes as disparate as myosin heavy chain, beta globin and adenovirus. The functional (and structural) role of introns remains uncertain, and although our discovery does not resolve the "intron-late" vs. "intron-early" controversy about gene evolution [55], it does reveal intriguing fractal properties of genome organization that need to be accounted for by any such theory.

Very recently, the idea of long-range correlations has been extended to the analysis of the beat-to-beat intervals in the normal and diseased heart [56].

8. Territory covered by N diffusing particles

The last topic I wish to discuss is an application of basic ideas of random walks to characterize the spread of a population. This concerns the solution of a hitherto unsolved problem of interest in physics, chemistry, metallurgy and, of course, ecology [57].

The mean number of distinct sites visited by a single random walker after a time t is a quantity of longstanding interest since it is a direct measure of the territory

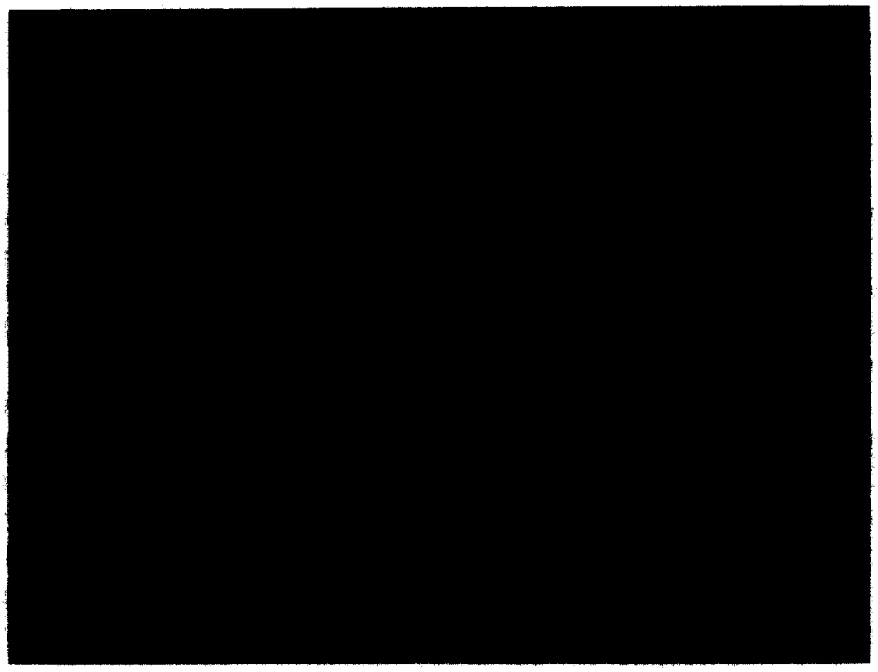

Fig. 18

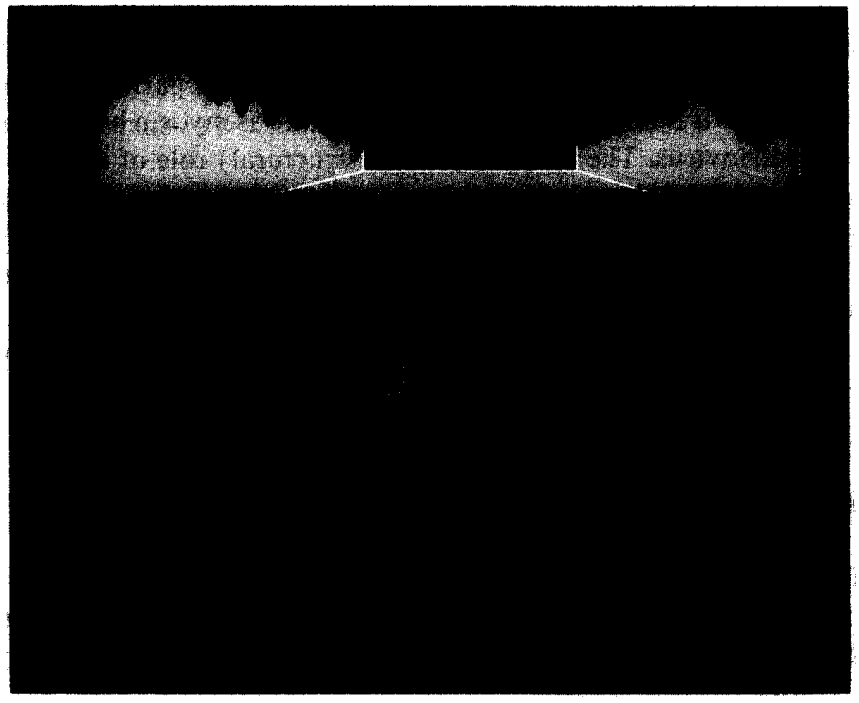

Fig. 19

covered by a diffusing particle. This quantity enters into the description of many phenomena of interest in ecology [58], metallurgy [59], chemistry [60], and physics [61]. Previous analysis [62] has been limited to the number of distinct sites visited by a *single* random walker, $S_1(t)$. The nontrivial generalization to $S_N(t)$, the mean number of distinct sites visited by N walkers, is particularly relevant to the classic problem in mathematical ecology of defining the territory covered by N members of a given species [58, 63] and is also related to the study of the Smoluchowski model for the rate of chemical reactions of the form $A + B \rightarrow B$, taking into account the possibility of a number of B's rather than the single B envisaged by Smoluchowski [60]. We have recently obtained an analytic solution to the problem of calculating $S_N(t)$ on a d-dimensional lattice, for $d = 1, 2, 3$. We have confirmed the analytic arguments by Monte Carlo and exact enumeration methods. We found three distinct time regimes, and we found $S_N(t)$ in each regime. Moreover we also found a remarkable transition in the actual geometry of the set of visited sites. This set initially grows with the shape of a disk with a relatively smooth surface until it reaches certain size, at which the surface becomes increasingly rough (see figs. 20 and 21). This phenomenon may have been observed by Skellam [63], who plotted contours delineating the advance of the muskrat population and noted that initially the contours were smooth but at later times they become rough (see fig. 1 of ref. [63]).

Fig. 18. The DNA walk representations of (top) intron-rich human β-cardiac myosin heavy chain gene sequence, (middle) its cDNA, and (bottom) the intron-less bacteriophage lambda DNA sequence. Note the more complex fluctuations for the intron-containing gene in (top) compared with the intron-less sequences (middle) and (bottom). Note the more complex fluctuations observed for the intron-containing gene in (top) as compared with the intron-less sequences (middle). The very jagged contour of the DNA walk in (top), characteristic of intron-containing genes, is associated with long-range correlations. After ref. [51].

Fig. 19. The DNA walk representation for the rat embryonic skeletal myosin heavy chain gene ($\alpha = 0.63$). (top) The entire sequence. (middle) The magnification of the solid box in (top). (bottom) The magnification of the solid box in (middle). The statistical self-similarity of these plots is consistent with the existence of a scale-free or fractal phenomenon which we call a fractal landscape. Note that one must magnify the segment by different factors along the ℓ (horizontal) direction and the y (vertical) direction; since F has the same units (dimension) as y, these magnification factors M_ℓ and M_y (along ℓ and y directions respectively) are related to the scaling exponent α by the simple relation $\alpha = \log(M_y)/\log(M_\ell)$ [e.g., from (top) to (middle), $\log(M_y)/\log(M_\ell) = \log(2.07)/\log(3.2) \cong 0.63$]. After ref. [51].

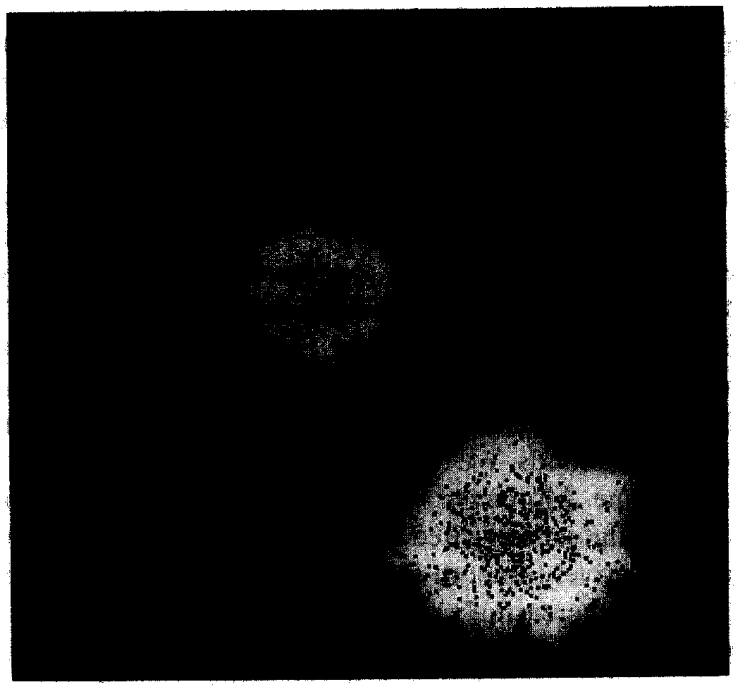

Fig. 20. Snapshots at successive times of the territory covered by N random walkers for the case $N = 500$ for a sequence of times. Note the roughening of the disc surface as time increases. The roughening is characteristic of the experimental findings for the diffusive spread of a population [63]. After ref. [57].

9. Concluding remarks

It is awe-inspiring that remarkably complex objects in nature can be quantitatively characterized by a single number, d_f. It is equally awe-inspiring that such complex objects can be described by various models with extremely simple rules. It is also an intriguing fact that even though no two natural fractal objects that we are likely to ever see are identical, nonetheless many fractals – such as DLA – have a generic 'form' that even a child can recognize (indeed, the teaching of recognizable structures that emerge "magically" from purely random motion (such as DLA) is finding its way into the school curriculum [64]). The analogous statement holds for many random structures in nature – e.g., no two snowflakes are the same yet every snowflake has a recognizable generic form.

Perhaps most awesome to a science student is the fact that geometrical models – with no Boltzmann factors – suffice to capture features of real statistical mechanical systems. What does this mean? If we understand the essential physics of an extremely robust model, such as the Ising model, then we say that we understand the essential physics of the complex materials that fall into the universality class described by the Ising model. In fact, by understanding the pure Ising

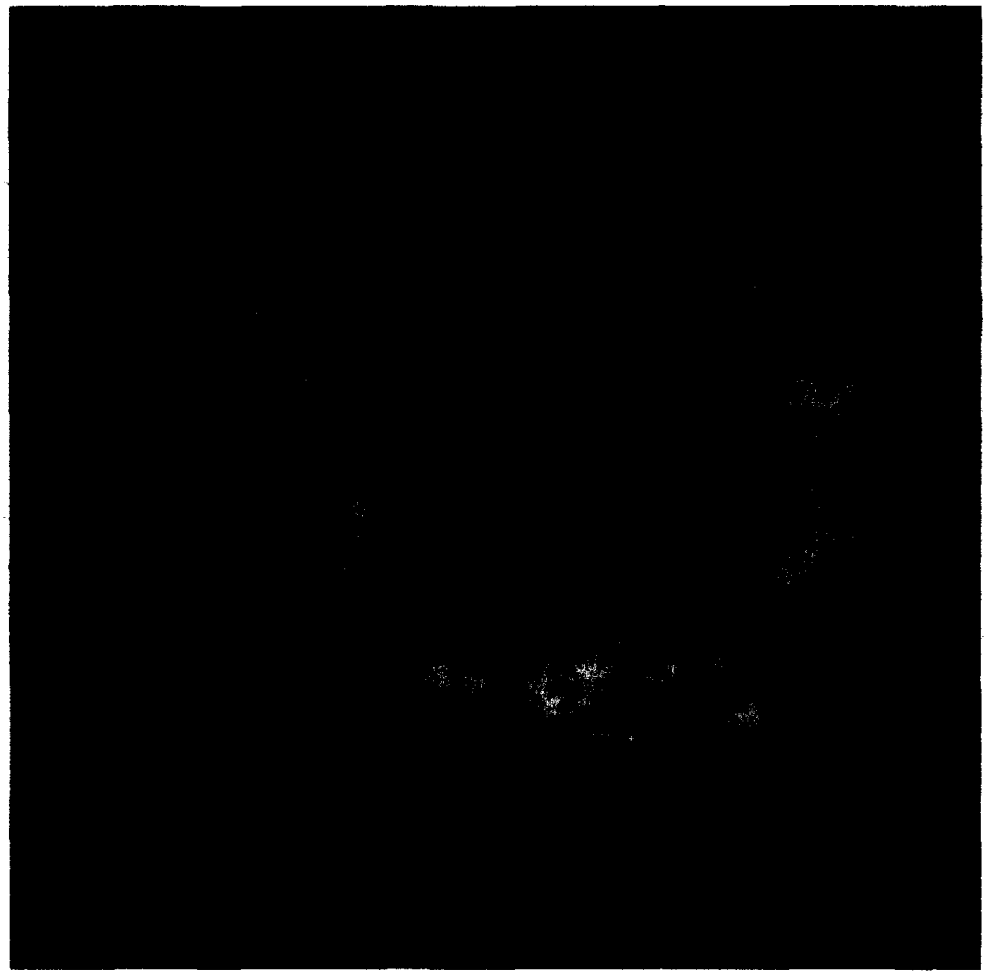

Fig. 21. Photograph showing a superposition of the territory covered by N random walkers at successive times. Note the roughening of the disc surface as time increases. Courtesy of P. Trunfio.

model, we can even understand most of the features of *variants* of the Ising model (such as the n-vector model) that may be appropriate for describing even more complex materials. Similarly, we feel that if we can understand DLA, then we are well on our way to understanding *variants* of DLA. And just as the Ising model is a paradigm for all systems composed of interacting subunits, so also DLA may be a paradigm for all kinetic growth models. As for biology, our hope is that some of the newer ideas of correlated spatial randomness [52], anomalous surface roughening [65], etc. that we and many other groups have been developing will prove useful in understanding the long-range correlations in intron nucleotide sequences [51] and the beat-to-beat correlations in the normal heart [56]. Also, we hope to better understand the nature of *realistic* surfaces; until now, most of our work is restricted to $1+1$ dimensions, but we are optimistic that novel visual-

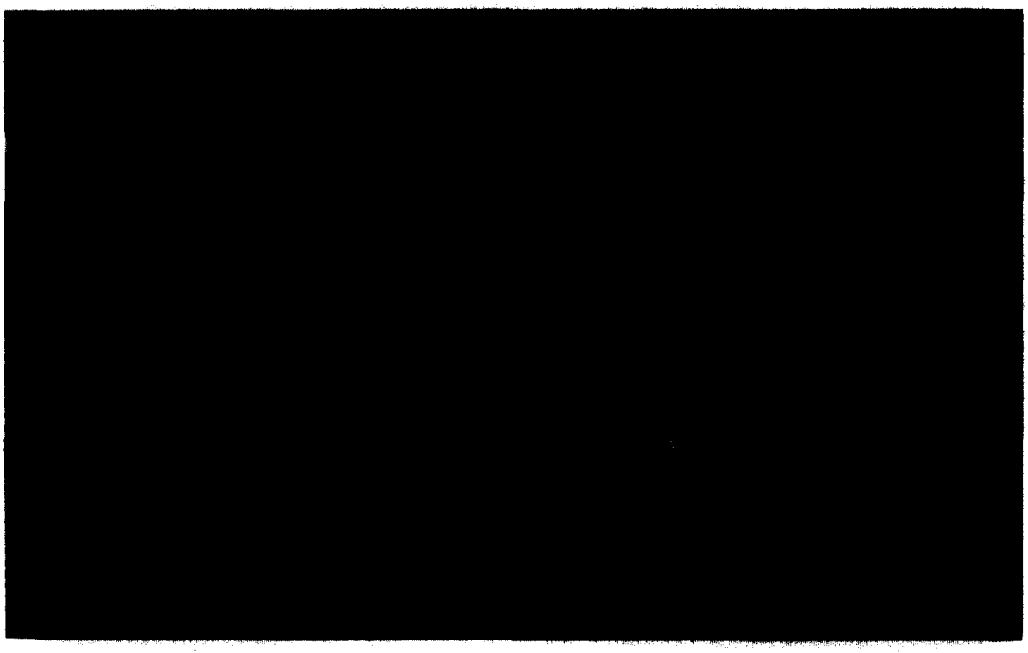

Fig. 22. Photographs showing the fashion in which a surface grows in dimension 2 + 1. The colors indicate the effective "elevation" of the surface, with white clouds indicating the highest elevation. Courtesy of S.V. Buldyrev.

ization techniques will lead to progress for the case of 2 + 1 dimensions (fig. 22).

The neuron example is particularly intriguing: if evolution indeed chose DLA as the morphology for the nerve cell, then can we understand "why" this choice was made? What evolutionary advantage does a DLA morphology convey? Is it significant that the Paris railway system evolved with the same morphology – even the same fractal dimension – or is this fact just a numerical coincidence? Can we use the answer to these questions to better design the next generation of computers? These are important issues that we cannot hope to resolve quickly, but already we appreciate that a fractal object is the most efficient way to obtain a great deal of intercell "connectivity" with a minimum of "cell volume", so the next question is "which" fractal did evolution select, and why? Is it worth our group's "all-out effort" [66] seeking a deep understanding of both the fractal and multifractal aspects of DLA, or should we be content with the present numerical description of the parameters characterizing this idealized model system?

Acknowledgements

I wish to thank all who have made possible my appreciation of fractal objects and their significance in many branches of science. First and foremost, I wish to thank Prof. Benoit Mandelbrot for introducing me to the subject in 1976 and for having patience with my feeble attempts at that time to interpret the geometry of percolation clusters in terms of fractal dimensions. Secondly, I wish to thank the many visitors to Boston who have given so generously of their time and of their ideas.

Most important, perhaps, I wish to acknowledge my collaboration with my students and with my colleagues.

The results discussed in this lecture benefited directly from work of many individuals, among whom are A. Aharony, P. Alstrøm, M. Araujo, A.-L. Barabási, K.R. Bhaskar, S.V. Buldyrev, A. Bunde, F. Caserta, A. Coniglio, G. Daccord, P. Devillard, Z. Djordjevic, A.D. Fowler, P. Garik, A. Geiger, S. Glotzer, A.L. Goldberger, E. Guyon, M.F. Gyure, A.B. Harris, S. Havlin, H.J. Herrmann, G. Huber, N. Jan, J. Kertész, H. Larralde, J. Lee, B.B. Mandelbrot, A. Margolina, P. Meakin, S. Milošević, T. Nagatani, H. Nakanishi, J. Nittmann, N. Ostrowsky, C.-K. Peng, P.H. Poole, P.J. Reynolds, S. Schwarzer, F. Sciortino, R.L. Blumberg Selinger, M. Simons, M. Schwartz, D. Stauffer, B. Stošić, P. Trunfio, T. Vicsek, G.H. Weiss and T.A. Witten.

Last but not least, I wish to thank ONR and NSF for financial support, without which none of this research could have taken place.

References

[1] B.B. Mandelbrot, The Fractal Geometry of Nature (Freeman, San Francisco, 1982).
[2] F. Family and D.P. Landau, eds., Kinetics of Aggregation and Gelation (Elsevier, Amsterdam, 1984).
[3] H.E. Stanley and N. Ostrowsky, eds., On Growth and Form: Fractal and Non-Fractal Patterns in Physics, Proc. 1985 Cargèse NATO ASI, Series E: Applied Sciences, vol. 100 (Nijhoff, Dordrecht, 1985).
[4] L. Pietronero and E. Tosatti, eds., Fractals in Physics (Elsevier, Amsterdam, 1986).
[5] N. Boccara and M. Daoud, eds., Physics of Finely Divided Matter (Springer, Berlin, 1986).
[6] R. Pynn and A. Skjeltorp, eds., Scaling Phenomena in Disordered Systems (Plenum, New York, 1986).
[7] R. Pynn and T. Riste, eds., Time Dependent Effects in Disordered Materials (Plenum, New York, 1987).
[8] R. Jullien and R. Botet, Aggregation and Fractal Aggregates (World Scientific, Singapore, 1987).
[9] J. Feder, Fractals (Plenum, New York, 1988).
[10] H.E. Stanley and N. Ostrowsky, eds., Random Fluctuations and Pattern Growth: Experiments and Theory, Proc. 1988 Cargèse NATO ASI Series E: Applied Sciences, vol. 157 (Kluwer, Dordrecht, 1988).

[11] T. Vicsek, Fractal Growth Phenomena (World Scientific, Singapore, 1989).
[12] D. Avnir (ed.), The Fractal Approach to Heterogeneous Chemistry (Wiley, Chichester, 1989).
[13] H. Takayasu, Fractals in the Physical Sciences (Manchester Univ. Press, Manchester, 1990).
[14] A.J. Hurd (ed.), Fractals – Selected Reprints (American Assoc. Phys. Teacher, College Park MD, 1989).
[15] B.H. Kaye, A Random Walk through Fractal Dimensions (VCH, Weinheim, 1989).
[16] J.P. Hulin, A.M. Cazabat, E. Guyon and F. Carmona, eds., F.Hydrodynamics of Dispersed Media, Random Materials and Processes, vol. 1 (North-Holland, Amsterdam, 1990).
[17] H.J. Herrmann and S. Roux, eds., Statistical Models for the Fracture of Disordered Media, Random Materials and Processes, vol. 2 (North-Holland, Amsterdam, 1990).
[18] H.E. Stanley and N. Ostrowsky, eds., Correlations and Connectivity: Geometric Aspects of Physics, Chemistry and Biology, Proc. 1990 Cargèse NATO ASI, Series E: Applied Sciences, vol. 188 (Kluwer, Dordrecht, 1990).
[19] A. Aharony and J. Feder, eds., Fractals in Physics: Essays in Honor of B.B. Mandelbrot (North-Holland, Amsterdam, 1990).
[20] L. Pietronero (ed.), Fractals: Physical Origin and Properties (Plenum, London, 1990).
[21] D. Stauffer and H.E. Stanley, From Newton to Mandelbrot: A Primer in Theoretical Physics (Springer, Berlin, 1990).
[22] E. Guyon and H.E. Stanley, Fractal Forms (Elsevier (North-Holland)/Palais de la Decouverte, Amsterdam/Paris, 1991) [French translation: les Formes Fractales].
[23] A. Bunde and S. Havlin, eds., Fractals and Disordered Systems (Springer-Verlag, Berlin, 1991).
[24] L. Benguigui and M. Daoud, Geograph. Anal. 23 (1991) 362.
[25] J. Perrin, Les Atomes (Alcan, Paris, 1915) [English Translation by D.L. Hammick, Atoms (Constable, London)].
[26] H.E. Stanley, J. Stat. Phys. 36 (1984) 843.
[27] T.A. Witten and L.M. Sander, Phys. Rev. Lett. 47 (1981) 1400.
[28] R.M. Brady and R.C. Ball, Nature 309 (1984) 225. M. Matsushita, M. Sano, Y. Hakayawa, H. Honjo, Y. Sawada, Phys. Rev. Lett. 53 (1984) 286.
[29] J. Nittmann and H.E. Stanley, Nature 321 (1986) 663.
[30] J. Nittmann, H.E. Stanley, J. Phys. A 20 (1987) L981.
[31] J. Nittmann, H.E. Stanley, J. Phys. A 20 (1987) L1185.
[32] L. Niemeyer, L. Pietronero and H.J. Wiesmann, Phys. Rev. Lett. 52 (1984) 1033; L. Pietronero, H.J. Wiesmann, J. Stat. Phys. 36 (1984) 909.
[33] H.S. Hele-Shaw, Nature 58 (1898) 34; P.G. Saffman and G.I. Taylor, Proc. R. Soc. London A 245 (1958) 312; J. Nittmann, G. Daccord, H.E. Stanley, Nature 314 (1985) 141; H. Van Damme, F. Obrecht, P. Levitz, L. Gatineau, C. Laroche, Nature 320 (1986) 731; G. Daccord, J. Nittmann and H.E. Stanley, Phys. Rev. Lett. 56 (1986) 336; U. Oxaal, M. Murat, F. Boger, A. Aharony, J. Feder, T. Jøssang, Nature 329 (1987) 32; R.B. Selinger, J. Nittmann and H.E. Stanley, Phys. Rev. A 40 (1989) 2590.
[34] G. Daccord, Phys. Rev. Lett. 58 (1987) 479; G. Daccord and R. Lenormand, Nature 325 (1987) 41; T. Nagatani, J. Lee and H.E. Stanley, Phys. Rev. Lett. 66 (1991) 616; Phys. Rev. A 45 (1992) 2471.
[35] A.D. Fowler, H.E. Stanley and G. Daccord, Nature 341 (1989) 134.
[36] M. Matsushita and H. Fujikawa, Physica A 168 (1990) 498.
[37] F. Family, B.R. Masters and D.E. Platt, Physica D 38 (1989) 98.
[38] F. Caserta, H.E. Stanley, W. Eldred, G. Daccord, R.E. Hausman, J. Nittmann, Phys. Rev. Lett. 64 (1990) 95; D. Kleinfeld, F. Raccuia-Behling, G.E. Blonder, Phys. Rev. Lett. 65 (1990) 3064; F. Caserta, R.E. Hausman, W.D. Eldred, H.E. Stanley and C. Kimmel, Neurosci. Lett. 136 (1992) 198; F. Caserta, W.D. Eldred, R.E. Hausman, L.R. Stanford and H.E. Stanley, Neurite outgrowth and fractal dimension, J. Neurosci. Meth., submitted.
[39] K.R. Bhaskar, B.S. Turner, P. Garik, J.D. Bradley, R. Bansil, H.E. Stanley and J.T. LaMont, Viscous fingering of HCl through gastric mucin, Nature, submitted.

[40] H.E. Stanley, Introduction to Phase Transitions and Critical Phenomena, 2nd ed. (Oxford Univ. Press, London), in press.

[41] D. Stauffer, Introduction to Percolation Theory (Taylor & Francis, London, 1985); A. Geiger and H.E. Stanley, Phys. Rev. Lett. 49 (1982) 1895; E.T. Gawlinski, H.E. Stanley, J. Phys. A 14 (1981) L291; A. Geiger and H.E. Stanley, Phys. Rev. Lett. 49 (1982) 1749; R.L.B. Selinger and H.E. Stanley, Phys. Rev. A 42 (1990) 4845.

[42] W. Lenz, Phys. Z. 21 (1920) 613; E. Ising, Ann. Phys. 31 (1925) 253.

[43] F. Sciortino, A. Geiger and H.E. Stanley, Phys. Rev. Lett. 65 (1990) 3452; F. Sciortino, P. Poole, H.E. Stanley and S. Havlin, Phys. Rev. Letters 64 (1990) 1686; F. Sciortino, A. Geiger and H.E. Stanley, Nature 354 (1991) 218; S. Sastry, F. Sciortino and H.E. Stanley, J. Chem. Phys. 95 (1991) 7775; F. Sciortino, A. Geiger and H.E. Stanley, J. Chem. Phys. 96 (1992) 3857.

[44] S.C. Glotzer, F. Sciortino, M. Gyure, R. Bansil and H.E. Stanley, Microphase separation in polymers: interference between thermoreversible gelation and spinodal decomposition, Nature, submitted; F. Sciortino, R. Bansil, H.E. Stanley and P. Alstrøm Interference of phase separation and gelation, Phys. Rev., submitted.

[45] E. Ben-Jacob et al., Phys. Rev. Lett. 55 (1985) 1315; E. Ben-Jacob and P. Garik, Nature 343 (1990) 523; J.S. Langer, Science 243 (1989) 1150; A. Buka, J. Kertész and T. Vicsek, Nature 323 (1986) 424.

[46] H.E. Stanley, Physica A 163 (1990) 334.

[47] U. Nakaya, Snow Crystals (Harvard Univ. Press, Cambridge, MA, 1954).

[48] E.R. LaChapelle, Field Guide to Snow Crystals (Univ. of Washington Press, Seattle, 1969).

[49] W.A. Bentley and W.J. Humphreys, Snow Crystals (Dover, New York, 1962).

[50] A. Dougherty, P.D. Kaplan and J.P. Gollub, Phys. Rev. Lett. 58 (1987) 1652.

[51] C.K. Peng, S.V. Buldyrev, A. Goldberger, S. Havlin, F. Sciortino, M. Simons and H.E. Stanley, Nature 356 (1992) 168; S.V. Buldyrev, M. Simons, C.K. Peng, A. Goldberger, S. Havlin and H.E. Stanley, Molecular evolution and fractal landscapes, preprint.

[52] S. Havlin, R. Selinger, M. Schwartz, H.E. Stanley, A. Bunde, Phys. Rev. Lett. 61 (1988) 1438; S. Havlin, M. Schwartz, R. Blumberg Selinger, A. Bunde and H.E. Stanley, Phys. Rev. A 40 (1989) 1717; R.B. Selinger, S. Havlin, F. Leyvraz, M. Schwartz and H.E. Stanley, Phys. Rev. A 40 (1989) 6755; C.K. Peng, S. Havlin, M. Schwartz and H.E. Stanley, Phys. Rev. A 44 (1991) 2239; C.K. Peng, S. Havlin, M. Schwartz, H.E. Stanley, G.H. Weiss, Physica A 178 (1991) 401; S. Prakash, S. Havlin, M. Schwartz and H.E. Stanley, Structural and Dynamical Properties of Long-Range Correlated Percolation, Phys. Rev. A (submitted).

[53] S. Tavaré and B.W. Giddings, in: Mathematical Methods for DNA Sequences, M.S. Waterman, ed. (CRC Press, Boca Raton, 1989), p. 117.

[54] E.W. Montroll and M.F. Shlesinger, The wonderful world of random walks, in: Nonequilibrium Phenomena II. From Stochastics to Hydrodynamics, eds. J.L. Lebowitz and E.W. Montroll (North-Holland, Amsterdam, 1984) p. 1–121.

[55] W. Gilbert, Nature 271 (1978) 501; J.E. Darnell, Jr., Science 202 (1978) 1257; W.F. Doolittle, Nature 272 (1978) 581.

[56] C.K. Peng, J. Mietus, J. Hausdorff, A.L. Goldberger, S. Havlin and H.E. Stanley, Nonequilibrium behavior of the heartbeat, Nature, submitted.

[57] H. Larralde, P. Trunfio, S. Havlin, H.E. Stanley and G.H. Weiss, Nature 355 (1992) 423; M.F. Shlesinger, Nature 355 (1992) 396; H. Larralde, P. Trunfio, S. Havlin, H.E. Stanley and G.H. Weiss, Phys. Rev. A 45 (1992) 7128; S. Havlin, H. Larralde, P. Trunfio, J.E. Kiefer, H.E. Stanley and G.H. Weiss, The number of distinct sites visited by N particles diffusing on a fractal, Phys. Rev. A (submitted); H. Larralde, P. Trunfio, S. Havlin and H.E. Stanley, Reaction kinetics of diffusing particles injected into a reactive medium, Phys. Rev. A (submitted).

[58] E.C. Pielou, An Introduction to Mathematical Ecology (Wiley–Interscience, NY, 1969); L. Edelstein-Keshet, Mathematical Models in Biology (Random House, New York, 1988).

[59] R.J. Beeler and J.A. Delaney, Phys. Rev.A 130 (1963) 926; R.J. Beeler, Phys. Rev. A 134 (1964) 1396; H.B. Rosenstock, Phys. Rev. A 187 (1969) 1166.

[60] M. v. Smoluchowski, Z. Phys. Chem. 29 (1917) 129; S.A. Rice, Diffusion-Controlled Reactions (Elsevier, Amsterdam, 1985).

[61] J.W. Haus and K.W. Kehr, Phys. Rep. 150 (1987) 263; S. Havlin and D. Ben-Avraham, Adv. Phys. 36 (1987) 695; J.-P. Bouchaud, A. Georges, Phys. Rep. 195 (1990) 127.

[62] M.N. Barber and B.W. Ninham, Random & Restricted Walks (Gordon & Breach, New York, 1970); H.C. Berg, Random Walks in Biology (Princeton Univ. Press, Princeton, 1983).

[63] J.G. Skellam, Biometrika 38 (1951) 196.

[64] H.E. Stanley, Physica D 38 (1989) 330; B. Ostrovsky, P.H. Poole, F. Sciortino, H.E. Stanley and P. Trunfio, in: Festschrift for Michael E. Fisher, E. Domany and D. Jasnow, eds., Physica A 177 (1991) 281; S.V. Buldyrev, P. Garik, S. Glotzer, G. Huber, T. Mekonen, R. Selinger, M.H. Shann, L.S. Shore, H.E. Stanley, D. Stauffer, E.F. Taylor, P. Trunfio and T. Udale, Das zufällige Universum: forschendes ernen für Wahrscheinlichkeit und Fraktale (Klett, Frankfurt, Germany, 1992); U. Essmann, S. Glotzer, M. Gyure, B. Ostrovsky, P.H. Poole, S. Sastry, S. Schwarzer, R. Selinger, M.H. Shann, L.S. Shore, H.E. Stanley, E.F. Taylor and P. Trunfio, Learning science through guided discovery: liquid water & molecular networks, in: From Phase Transitions to Chaos: Topics in Modern Statistical Physics, G. Györgyi, I. Kondor, L. Sasvári and T. Tél, eds. (World Scientific, Singapore, 1992).

[65] S.V. Buldyrev, S. Havlin, J. Kertész, H.E. Stanley and T. Vicsek, Phys. Rev. A 43 (1991) 7113; S. Havlin, S.V. Buldyrev, H.E. Stanley and G.H. Weiss, J. Phys. A 24 (1991) L925; S.V. Buldyrev, A.-L. Barabási, F. Caserta, S. Havlin, H.E. Stanley and T. Vicsek, Phys. Rev. A 45 (1992) R-8313; L.-H. Tang and H. Leschhorn, Phys. Rev. A 45 (1992) R-8309; S.V. Buldyrev, A.-L. Barabási, S. Havlin and H.E. Stanley, Experiments on anomalous interface roughening in 2+1 dimensions, preprint; G. Huber, S.V. Buldyrev, S. Havlin and H.E. Stanley, Rough surfaces and directed percolation, preprint; A.-L.Barabási, S.V. Buldyrev, S. Havlin, G. Huber, H.E. Stanley and T. Vicsek, Imbibition in porous media: experiment and theory, in: Proc. Les Houches Workshop (March 1992), R. Jullien, J. Kertész, P. Meakin and D.E. Wolf, eds. (Nova Science, N.Y., 1992).

[66] A. Coniglio and H.E. Stanley, Phys. Rev. Lett. 52 (1984) 1068; P. Meakin, H.E. Stanley, A. Coniglio and T.A. Witten, Phys. Rev. A 32 (1985) 2364; P. Meakin, A. Coniglio, H.E. Stanley and T.A. Witten, Phys. Rev. A 34 (1986) 3325; H.E. Stanley and P. Meakin, Nature 335 (1988) 405; H.E. Stanley, A. Bunde, S. Havlin, J. Lee, E. Roman, S. Schwarzer, Physica A 168 (1990) 23; S. Schwarzer, J. Lee, A. Bunde, S. Havlin, H.E. Roman, H.E. Stanley, Phys. Rev. Lett. 65 (1990) 603; P. Trunfio and P. Alstrøm, Phys. Rev. B 41 (1990) 896; J. Lee, S. Havlin, H.E. Stanley and J. Kiefer, Phys. Rev. A 42 (1990) 4832; P. Alstrøm, P. Trunfio and H.E. Stanley, Phys. Rev. A Rapid Commun. 41 (1990) 3403; S. Schwarzer, J. Lee, S. Havlin, H.E. Stanley and P. Meakin, Phys. Rev. A 43 (1991) 1134; J. Lee, S. Havlin and H.E. Stanley, Phys. Rev. A 45 (1992) 1035; J. Lee, A. Coniglio and H.E. Stanley, Localization of growth sites in DLA clusters: multifractality and multiscaling, Nature, submitted. S. Schwarzer, M. Wolf, S. Havlin, P. Meakin and H.E. Stanley, Multifractal spectrum of three-dimensional diffusion limited aggregation, Phys. Rev. A, submitted; S. Schwarzer, S. Havlin and H.E. Stanley, Internal structure of diffusion limited aggregation, Phys. Rev. A, submitted.